A RESHAPED GABOR CUSTOMIZED CONVOLUTIONAL NEURAL NETWORK FOR RESTORATION AND ENHANCEMENT OF BRAIN MR IMAGES

Vinay Kumar[1]* and Subodh Srivastava[2]

Article History: **Received: 02/08/2023** **Revised: 05/08/2023** **Accepted: 15/08/2023**

Abstract

Magnetic resonance imaging is the clinically acclaimed imaging modalities which is utilized for the screening of brain abnormalities. It provides the visual interpretation of the abnormalities in terms of tumors, masses, grey matter and clots. However, these readable features of brain are affected due to the presence of inherent Rician noise. Moreover, it also restricts the decision capability of the expert about the brain abnormalities. So, for the restoration and enhancement the brain MR images, a Reshaped Gabor filter based Convolution neural network (RGCNN) method is proposed. In order to develop the proposed RGCNN, a Gabor Layer is employed as the initial layer within a deep convolutional network. This modification provides a better correlation amid the noisy pixel The efficacy of the proposed method has been assessed with respect to the qualitative and quantitative assessment for the brain web dataset. The human visual system, full and no reference image metrics are used to quantitatively measure the performance of the proposed method. Apart from this, a comparative study has been also presented between the proposed and existing method to describe the effectiveness of the proposed method. The obtained results demonstrate that the proposed method is capable of simultaneously reducing Rician noise, preserving edges, restoring fine details, and enhancing anomalies.

Keywords: Brain, Magnetic Resonance Imaging, Reshaped Gabor Filter, Enhancement, CNN, Restoration

[1]*, [2]Department of Electronics and Communication Engineering, National Institute of Technology, Patna, Patna, 800005, E-mail:- vinay.ec17@nitp.ac.in[1]*, subodh@nitp.ac.in[2]

***Corresponding Author: -** Vinay Kumar
Department of Electronics and Communication Engineering, National Institute of Technology, Patna, Patna, 800005, E-mail:- vinay.ec17@nitp.ac.in

DOI: - 10.48047/ecb/2023.12.si10.00519

1. Introduction

The brain screening provides the structural overview as well as changes in the brain functionalities[1]. It describes the brain disorder and conditions in terms of abnormalities such as grey matter particles, tumors, clots and masses. Epilepsy, schizophrenia, autism, Parkinson's, stroke, and dementias are the most common types of neurological illnesses affecting the brain[2]. These disorders are raised due the alteration in the shape of brain cells. The incidence and mortality rate by of brain disorder are increasing day to day. It can be only prevented by the early diagnosis of the disorder.

Magnetic resonance imaging (MRI) is the widely used imaging tool for the diagnosis of brain disorders[3]. It is popular due to its non-invasive property and less radiative nature. It concurrently uses a magnetic field and radio waves simulated via computer to obtain the raw images of brain cells. The produced raw images are complex-valued in nature and for the better visualization it is transformed into the magnitude valued image with the aid of mathematical operations[4]. However, the acquired images have low signal-to-noise-ratio that confirms the existence of noise in the image. The origin of noise varies from one source to other. The prominent sources of noise include machine's calibration, sensors, coils, environment illumination, acquisition, transmission, and storage medium[5]. Literature shows that the MR magnitudes image generally comply to the Rician noise [6], [7]. It is an undesired inherent characteristic of the image which is multiplicative in nature. It affects both the image's readability features and clarity of the image. It confines the exact interpretation of the diseases by the experts. Moreover, it reduces the high frequency as well as the fine detail information of the image such as edges and boundary. Thus, the brain image restoration and enhancement are the two major concern that should be addressed properly for the early diagnosis of brain disorder.

To achieve the restoration and enhancement of brain MR images in a single framework, a Reshaped Gabor based Convolution Neural Network has been proposed. It combines the attributes of reshaped Gabor filter[6] and Convolution neural network[8] for the image denoising and quality improvement respectively. In conventional CNN the first layer are filters. Which are called kernels. These kernels are replace by Reshaped Gabor filter kernel. Furthermore it is applied on MR data sets.

The rest of the paper has been systematized as follows: section 2 reports the literature of existing denoising methods in contrast to MRI images. Section 3 illustrates about the used dataset and the proposed methodology. Section 4 presents the information of the performance assessment metrics in terms of human visual system, full and no reference image metric. Section 5 describes the performance of the proposed RGCNN. In addition, section 6 presents an overall conclusion.

2. Literature Survey

There has been various method developed to alleviate the negative impact of the Rician noise. It skews the exact position of brain lesions and makes medical diagnosis less precise. The denoising approaches for Rician noise have been widely classified as spatial, transform, similarity, and partial differential equation (PDE) based filters [9]. The mostly used spatial domain-based filter are median and wiener filter respectively. Gabor filter [6] and wavelet method lies under the transform domain denoising filter. The similarity based denoising filters comprises non-local means [10] and its modified form [11]. Furthermore, PDE-based techniques for MRI image denoising include total variation [12], anisotropic diffusion [13], complex diffusion [14],[15] and fourth order partial differential equation [7]. Apart from this, some of the methods follows the image enhancement after the image denoising.

Lee et al. [16] had used the properties of median and wiener filter for the denoising of T1 weighted brain MR images of the brain web dataset. The performance was illustrated with correspond to qualitative and quantitative assessment such as edge preservation index and coefficient of variation. Redhya et al. [15] had utilized adaptive median filter to minimize the noise from brain MR images. The work was primarily developed for the classification of Parkinson diseases. The image quality assessment parameters like mean square error (MSE), image enhancement factor and peak-signal-to-noise-ratio (PSNR) were estimated to judge the effectiveness of the method. Singh et al. [17] had compared the performance of median, Gaussian and wiener filter for the denoising of brain MR images. The efficacy was judged with respect to MSE and PSNR image metric. Ali et al [18] had employed mixing concatenation residual network (MCR) for the Gaussian and salt-pepper noise elimination from brain MR images. In this method six consecutive convolutional layers with the rectified linear unit (ReLU) were used for the denoising of image. The metrics such as structural

similarity index map (SSIM), PSNR and SSIM was determined as image quality assessment parameters. Kumar et al. [19] had clubs the PDE based anisotropic diffusion and unsharp masking for the noise removal of brain MR images. The method effectiveness was judged for MSE, PSNR, SSIM, correlation parameter (CP), and blind reference image spatial quality evaluator respectively. Yadav et al. [14] had used the other PDE rooted method i.e., complex diffusion for the elimination of Rician noise from MR images. In this method the image was treated as a complex-valued object, where the real and imaginary parts correspond to the intensity and gradient of the image respectively. The method efficacy was estimated for brain-web dataset and the metrics such MSE, PSNR, CP and SSIM were used for assessment purpose. Zhang et al. [14] had employed total-variation for the restoration of brain MR images. The method combines Fischer Burmeister function to regularize the total variation. The method effectiveness was evaluated in terms of MSE, PSNR and SSIM. Thakur et al. [20] had compared the working capability of denoising filters such as NLM, block matching three-dimensional filter, weighted nuclear norm minimization and fast Fourier transform. All of these approaches were tested on MR images and assessment metrics like PSNR and SSIM were analyzed. Kollem et al. [21] had used FPDE and quaternion wavelet transform for the noise removal from the MR images. The method uses a diffusivity function to advance the characteristic of PDE. PSNR, SSIM and MSE were evaluated to measure the performance of the method. Dinh [22] had combined the attributes of contrast limited adaptive histogram equalization, denoise convolutional neural network, Laplacian edge detector and marine predators' algorithm respectively for the removal of noise and enhancement of medical image. The method effectiveness was determined in terms of entropy, average gradient, and mean light intensity. Kumar et al. [6] had applied a reshaped Gabor filter for the denoising of MR images. The qualitative as well as quantitative assessment was performed to measure the efficacy of method.

The method such as AD [12] and CD [8] have an issue of over smoothening which obscures fine details. The method based on MF [9], WF [17] and GF [11] produces a low contrast image and fails to eliminate the noise. Furthermore, the methods like TV [14], and NLM [21] have limited performance in contrast to edge or high frequency information preservation. Thus, the main drawbacks of the current approaches can be understood from the reported literature in terms of excessive smoothing, edge blurring, loss of high frequency information and the formation of low contrast images. Therefor a Reshaped Gabor Filter based customized CNN has been proposed to address these problems.

3. Research Methodology

This section introduces a modified convolutional neural network (CNN) that utilizes a reshaped Gabor kernel. A standard convolutional neural network (CNN) is an algorithm that is driven by input and aims to build robust representations. However, this process often requires training a large number of parameters, also known as weights. Furthermore, the convergence of a neural network is contingent upon the initialization of its parameters. Typically, the weights are initialized using either a uniform or normal distribution. However, this issue leads to the convergence problem and poses challenges in training deep Convolutional Neural Networks (CNNs).

Gabor filters are extensively employed in the field of computer vision [6]. The sinusoidal plane wave with a specific frequency and orientation serves as the foundation for these methods, enabling them to extract spatial frequency structures from images [6]. Moreover, it has been demonstrated that these filters are suitable for applications involving texture representation and face detection [10]. Several studies have investigated the utilization of Gabor filters within Convolutional Neural Networks (CNNs). In a previous study [6], Gabor filters were employed as a pre-processing technique to generate Gabor features. These features were subsequently utilized as input to a convolutional neural network (CNN). Another study [7] implemented a constant Gabor filter bank as either the first or second layer of the CNN. This approach effectively reduced the number of trainable parameters within the network. Additionally, a novel concept of Convolutional Gabor orientation Filters was introduced in a subsequent study [11]. This unique structure modulates convolutional layers with learnable parameters, while incorporating a non-learnable Gabor filter bank. Nevertheless, the authors failed to document the incorporation of the filter parameters into the backpropagation process.

In this part, a Gabor Layer is employed as the initial layer within a deep convolutional network. The Gabor Layer is a type of convolutional layer that imposes constraints on its filters to conform to Gabor functions, often known as Gabor filters. The

initialization of filter parameters is based on the filter bank provided in reference [9]. Throughout the training phase, these parameters are changed using the usual backpropagation technique. The objective of this strategy is to enhance the resilience of acquired feature representations and minimise the training intricacy of neural networks. The Gabor Layer is incorporated into the fundamental components of Convolutional Neural Networks (CNNs) and can be seamlessly integrated into various deep CNN architectures.

3.1 Reshaped Gabor Filter

Gabor filter was used in various image processing application such as segmentation of texture, detecting targets, managing fractal dimension, analysis of document, detecting edges, retinal recognition, coding of image etc. [6]. Here we using Gabor filter for denoising purpose by making trails of control parameters. A block diagram of 2D Gabor filter is shown in Figure 1 and mathematically it is given as:

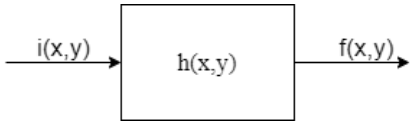

Figure 1: Gabor Filter block diagram

$$h(x,y) = g(x,y)exp[-j2\pi(Ux+Vy)] \quad (1)$$

And

$$g(x,y) = \frac{1}{2\pi\sigma^2} exp[-\frac{(x^2+y^2)}{2\sigma^2}] \quad (2)$$

Where i(x,y) is input noisy image given to Gabor filter with impulse response h(x,y) and f(x,y) is the filtered image. The impulse response h(x,y) also called Gabor function, which is formed by modulating a Gaussian kernel g(x,y) with a complex exponential or sinusoidal function. A detail explanation of Gabor filter is given by [6]. The output image f(x, y) of Gabor filter is given as:

$$f(x,y) = h(x,y) * i(x,y) \quad (3)$$

Where $*$ represents convolution in two dimensions. Since f(x,y) is complex valued image, then magnitude m(x,y) of image is given as:

$$m(x,y) = |f(x,y)| = |h(x,y) * i(x,y)| \quad (4)$$

3.2 Conventional CNN

Convolutional neural networks are commonly depicted as a series of many convolutional layers and fully linked layers, wherein a non-linear activation function is applied to the output of each layer. In order to mitigate the issue of overfitting, it is common practise to incorporate pooling and dropout layers inside the design. Convolutional layers optimise memory utilisation and enhance computational efficiency by employing identical filters over every pixel of the image. Figure 1 illustrates the conventional design of a Convolutional Neural Network (CNN).

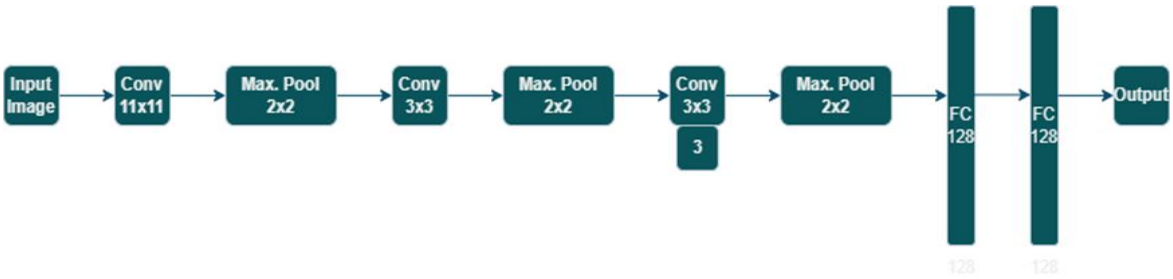

Figure 2: A conventional CNN

The training procedure of Convolutional Neural Networks (CNNs) typically involves the utilisation of the backpropagation algorithm [10]. This approach iteratively computes the gradient values for the weight coefficients situated across several layers. The weight update is subsequently executed with several iterations of stochastic gradient descent (SGD) techniques. Frequently, a family of first-order adaptive stochastic gradient descent (SGD) methods is employed [11] [12]. Therefore, it is necessary to impose constraints on the generating function of the convolutional layer, such as monotonicity and differentiability.

3.3 Proposed Reshaped Gabor CNN

Reference [6] provides a comprehensive understanding of Gabor filters and their process of reshaping. This section provides an explanation of the utilisation of Gabor kernels in Convolutional Neural Networks (CNNs). Gabor filters have demonstrated their efficacy as a valuable tool for extracting spectral information that are spatially localised, and are widely utilised in a range of pattern analysis applications [5]. The study conducted in reference [11] demonstrated that a deep convolutional neural network (CNN) trained on real-life images exhibits a tendency for the initial convolutional layers to predominantly learn

Gabor-like filters. The filters of the initial layers of a traditional Convolutional Neural Network (CNN) are depicted in Figure 3. This finding supports the notion of employing Gabor filters as the initial layer in a Convolutional Neural Network (CNN).

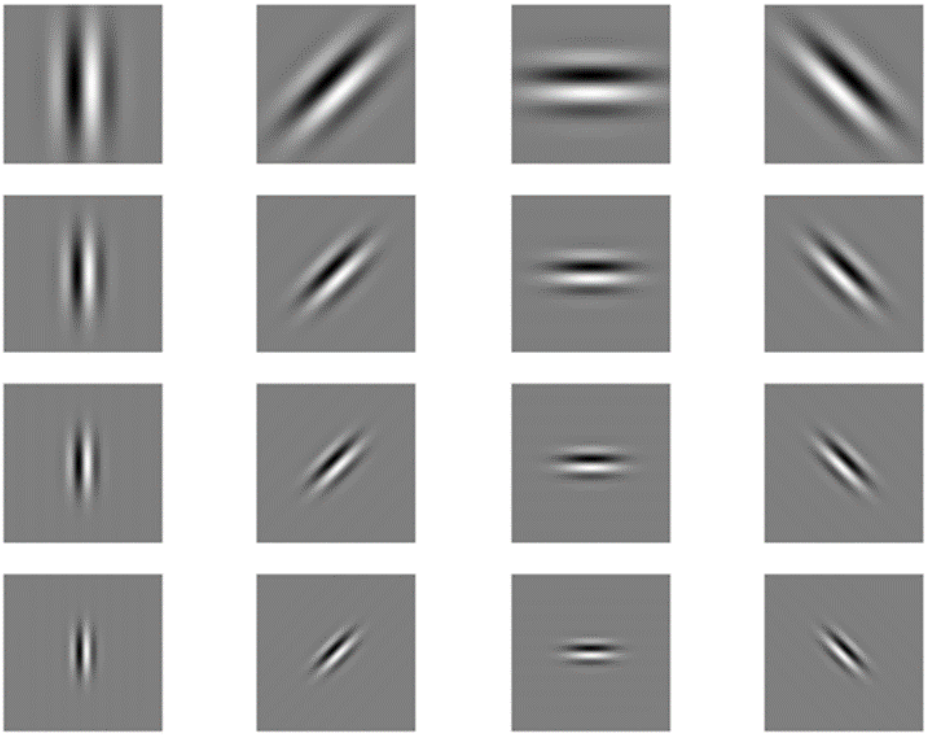

Figure 3. Gabor filter kernels of size 11x11

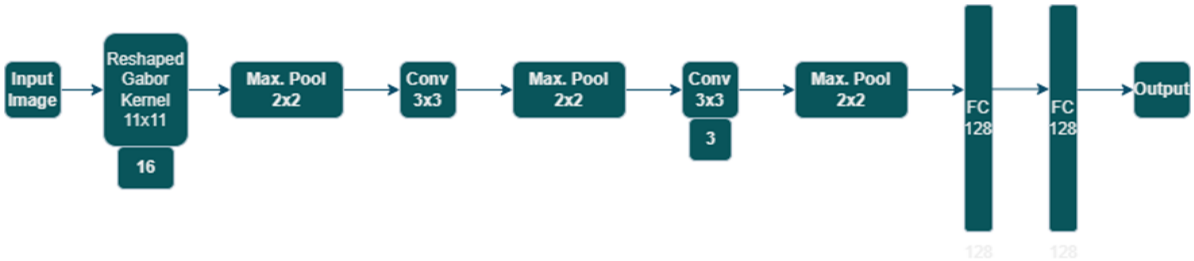

Figure 4. Proposed Reshaped Gabor Based Customized CNN

3.4 Dataset Collection

To develop the proposed method RGCNN, brain web [23] dataset has been collected. An openly accessible database is used as a benchmark data for the research work. The complete description of the database is given in Table 1.

Table 1: Information of the Brain Web Database

Key	Description
Imaging modalities	T1, T2, and PD
Types of noise variance	0%, 3%, 5%, 7% and 9%
Total Number of images	905 for each imaging modality
Image storage format	Portable Network Graphics (PNG)
Accessibility	Publicly
Size of image	181×127 Pixel

3.5 Performance Evaluation Metrics

The proposed RGCNN efficacy has been measured using multiple performance evaluation metrics. The metrics are divided with respect to human visual system [24], full and no reference image quality assessment measures. Table 2 depicts the mathematical formulation of the measures used.

Table 2: Performance Evaluation Metrics

Metrics		Mathematical Notation
Full reference Assessment Parameters (FRAP) [25]	Mean-Squared Error (MSE)	$MSE = \frac{1}{MN}\sum_{i=0}^{M-1}\sum_{j=0}^{N-1}[u(i,j) - I_{RDE}(i,j)]^2$
	Peak Signal-to-Noise Ratio (PSNR)	$PSNR = 10\log_{10}\frac{(L-1)}{MSE}db$
	Correlation Parameter (CP)	$CP = \frac{\sum(u(i,j)-\mu_u)\sum(I_{RDE}(i,j)-\mu_{I_{RDE}})}{\sqrt{\sum(u(i,j)-\mu_u)^2\sum(I_{RDE}(i,j)-\mu_{I_{RDE}})^2}}$
	Normalized Absolute Error (NAE)	$NAE = \frac{\sum_{i=0}^{M-1}\sum_{j=0}^{N-1}\lvert u(i,j) - I_{RDE}(i,j)\rvert}{\sum_{i=0}^{M-1}\sum_{j=0}^{N-1}u(i,j)}$
Human visual system Assessment Parameters (HVSAP) [24]	Universal Quality Index (UQI)	$UQI = \frac{4\mu_u\mu_{I_{RDE}}\sigma_{uI_{RDE}}}{(\mu_u{}^2 + \mu_{I_{RDE}}{}^2)(\sigma_u{}^2 + \sigma_{I_{RDE}}{}^2)}$ here, $\sigma_{uI_{RDE}} = \frac{1}{MN-1}\sum_{i=0}^{M-1}\sum_{j=0}^{N-1}(u(i,j)-\mu_u)(I_{RDE}(i,j)-\mu_{I_{RDE}})$
	Structural Similarity Index (SSIM)	$SSIM = \frac{(2\mu_u\mu_{I_{RDE}} + C_1)(2\sigma_{uI_{RDE}} + C_2)}{(\mu_u{}^2 + \mu_{I_{RDE}}{}^2 + C_1)(\sigma_u{}^2 + \sigma_{I_{RDE}}{}^2 + C_2)}$
No reference Assessment Parameters (NRAP) [25]	Perceptual Sharpness Index (PSI)	$I_{PSI}(i,j) = \begin{cases} \frac{I_{up}(i,j) - I_{down}(i,j)}{\cos(\Delta\emptyset(i,j))} - \frac{I_{max}(i,j) - I_{min}(i,j)}{I(i,j)}; & if\ \frac{I_{up}(i,j) - I_{down}(i,j)}{\cos(\Delta\emptyset(i,j))} \geq I_{jnb} \\ \frac{I_{up}(i,j) - I_{down}(i,j)}{\cos(\Delta\emptyset(i,j))}; otherwise \end{cases}$

Where u and I_{RDE} are the reference image and resultant image of RGCNN respectively. σ^2 and μ are the variance and mean of the corresponding image.

4 Results and Discussion

Both networks underwent training for a total of 100 epochs. The learning rate was initialised at 0.001, and the values for the betas were set to 0.9 and 0.999, respectively. The findings are depicted in Figure 5 (a) and (b). The results indicate that the Reshaped Gabor Convolutional Neural Network (RGCNN) has superior performance compared to the conventional Convolutional Neural Network (CNN), and it achieves convergence at earlier epochs. The final accuracy achieved by the performance gap is 6%. A comprehensive breakdown of the performance of GCNN and CNN can be seen in Table 3.

Table 3: Comparison of accuracy of Conventional CNN and proposed Gabor CNN

	Train		Test	
Epoch	CNN	GCNN	CNN	GCNN
1	0.402	0.501	0.401	0.522
5	0.512	0.534	0.504	0.531
10	0.531	0.552	0.521	0.541
15	0.542	0.573	0.532	0.557
20	0.556	0.592	0.551	0.572
40	0.603	0.627	0.594	0.609
50	0.621	0.689	0.611	0.621
60	0.657	0.694	0.631	0.652
70	0.689	0.723	0.652	0.688
80	0.721	0.751	0.661	0.702
90	0.732	0.762	0.710	0.731
100	0.751	0.798	0.725	0.752

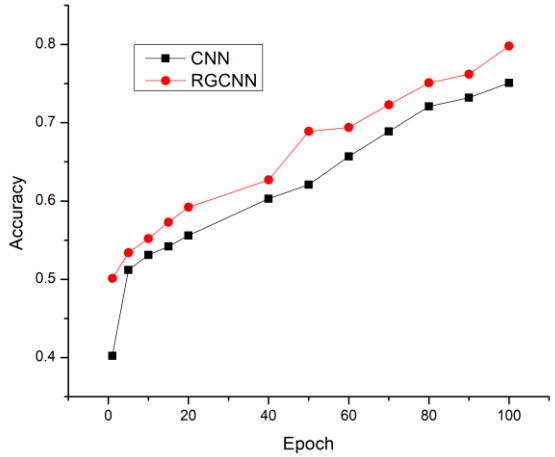

Figure 5(a): Performance of CNN and RGCNN for Training MRI data Sets

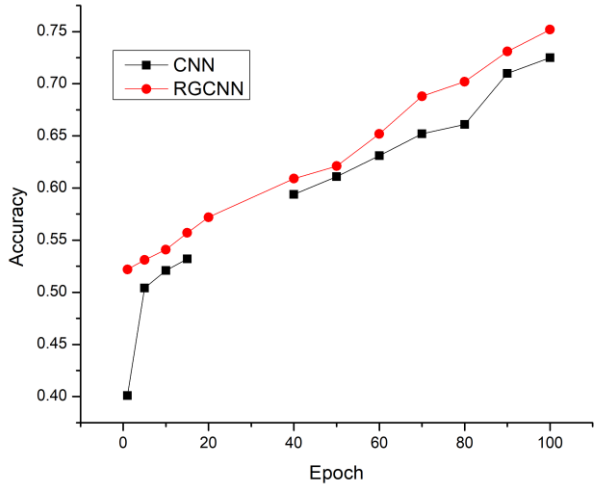

Figure 5 (b): Performance of CNN and RGCNN for Test MRI data Sets

5.1Qualitative assessment:

The improvement in image quality is measured with the aid of qualitative analysis. To perform the analysis T1, T2 and PD MRI images has been used with respect to the 9% noise variance. However, the process of evaluation stands same for the other noise variances such as 3%, 5%, and 7% of T1, T2 and PD brain MR images. Figure 6 exhibits the result of all steps involved during the implementation of proposed RGCNN for T1 MRI brain images. It comprises of total three images where (a) correspond to sample image; (b) is the noisy form of the sample image; and (c) is the restored, denoised and enhanced image obtained by the proposed method. Furthermore, Figures 7 demonstrates the qualitative result for T2 weighted MR image with 9% noise variance. The very first image i.e., (a) refers to sample input image; the second image i.e., (b) is the noisy image; and the last image i.e., (c) is the restored, denoised and enhanced image attained by the proposed RGCNN. In similar way, figure 8 exhibits the qualitative result for PD weighted MR image with 9% noise variance. The image (a) refers to sample input image; the image (b) is the noisy image; and the last image (c) is the restored, denoised and enhanced image attained by the proposed method. Figure 9 shows the illustrative comparative qualitative assessment. The comparison is evaluated with 9% noise variance of T1 MRI brain image. In these figures, image (a) to (i) are the resultant images of FPDE[26], NLM [20], WF [17], MCD [27], TV [12], ADMF [15], MCR [18], ADF [13], Gabor [6] and Proposed RGCNN respectively.

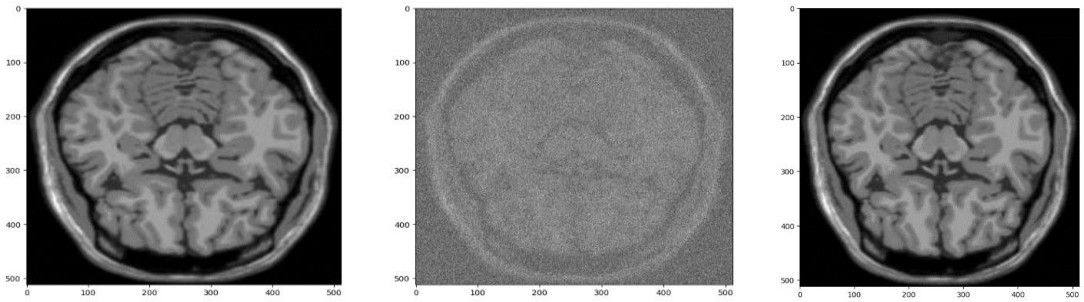

(a) (b) (c)

Figure 6: Result of proposed method for T1 weighted MR image (a) Noiseless image (b) Noisy Image (c) Output image RGCNN

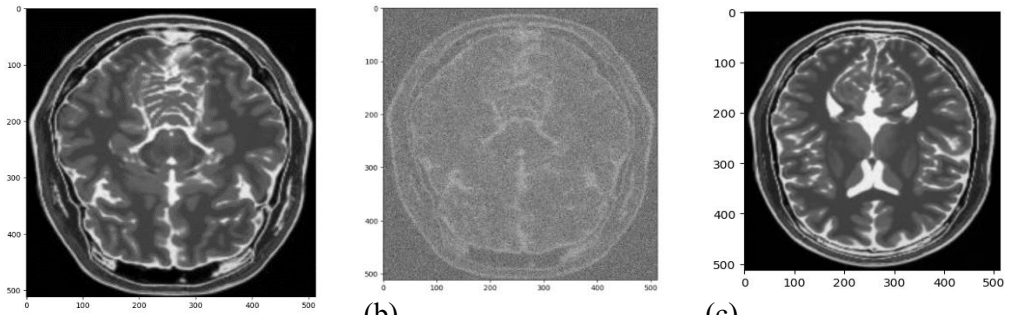

(a) (b) (c)

Figure 7: Result of proposed method for T2 weighted MR image (a) Noiseless image (b) Noisy Image (c) Output image by RGCNN

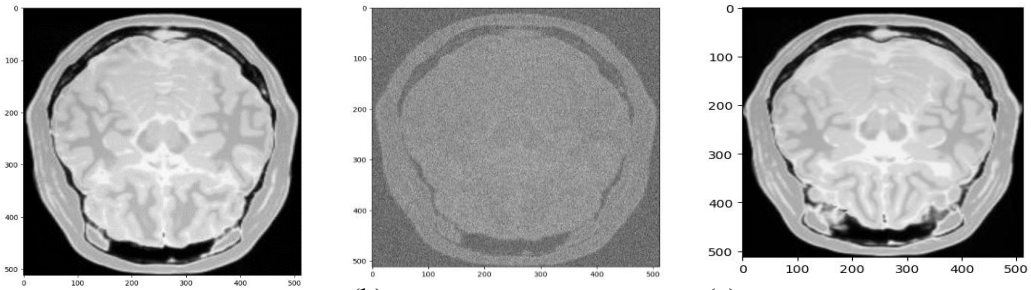

(a) (b) (c)

Figure 8: Result of proposed method for PD weighted MR image (a) Noiseless image (b) Noisy Image (c) Output image by RGCNN

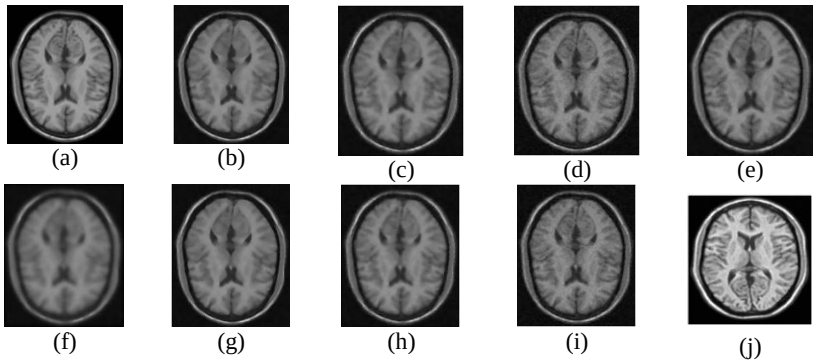

(a) (b) (c) (d) (e)

(f) (g) (h) (i) (j)

Figure 9: The output pictures acquired by the proposed method and other ways that already exist for T1 weighted MR image where (a) FPDE[26], (b) NLM [20], (c) WF [17], (d) MCD [27], (e) TV [12], (f) ADMF [15], (g) MCR [18], (h) ADF [13], (i) Gabor [6] and (j) Proposed RGCNN

5.2Quantitative assessment:

The performance of the proposed RGCNN has been assessed with the aid of quantitative analysis. It judges and compares the proposed method's efficacy with other existing methods in terms of numeric value. The values are obtained by

implementing the performance assessment parameters as mentioned in section 4. The quantifiable analysis has been calculated for the entire images of dataset. The comparative quantitative includes the results of FPDE[26], NLM [20], WF [17], MCD [27], TV [12], ADMF [15], MCR [18], ADF [13] and Gabor [6] filters which is reported in literature.

Table 3, 4 and 5 demonstrate the comparative numerical evaluation between the proposed and other existing methods for T1, T2 and PD brain respectively. It includes the performance assessments parameters of FRAP, HVSAP, and NRAP respectively. From the Table 3, the values of metrics such as MSE, PSNR, CP, NAE, UQI and SSIM and PSI have the following numeric scores of the proposed method 0.0227, 63.4917, 0.9465, 0.7429, 0.4423, 0.7242 and 0.6752 respectively. Tables 4 shows the comparative quantitative result for the entire images of 9% noise variance of T2 dataset with the following values MSE, PSNR, CP, NAE, UQI, SSIM and PSI respectively 0.0337, 67.8120, 0.9439, 0.9332, 0.6418, 0.0.4923 and 0.6782 respectively. Table 5 shows the quantitative result of PD MRI images. The numeric values of MSE, PSNR, CP, NAE, UQI, SSIM and PSI are 0.0551, 65.2952, 0.9432, 0.8991, 0.8592, 0.5395 and 0.8954 respectively. The comparative graphic line plot of Table 3, 4 and 5 is illustrated by Figure 10, 11 and 12 respectively.

Table 4: Comparative quantitative evaluation amid the reported methods and proposed RGCNN for T1 Brain MR image with 9% noise variance

Methods	**Parameters**						
	MSE	PSNR	SSIM	UQI	CP	NAE	PSI
FPDE[26]	0.3210	27.1439	0.6352	0.4367	0.3092	0.7892	0.3762
NLM [20]	0.4792	24.156	0.6425	0.4527	0.3189	0.7712	0.3216
WF [17]	0.3287	26.5492	0.6782	0.4732	0.3026	0.7737	0.3792
MCD [27]	0.7921	22.456	0.6621	0.4623	0.3153	0.8032	0.3498
TV [12]	0.3162	24.1567	0.7254	0.4713	0.2915	0.7752	0.6725
ADMF [15]	0.3526	26.8927	0.7692	0.4727	0.3691	0.7052	0.3215
MCR [18]	0.5726	23.456	0.7689	0.5556	0.3793	0.7792	0.3494
ADF [13]	0.5826	23.2621	0.5142	0.5681	0.4013	0.7952	0.3215
Gabor [6]	0.0798	58.9215	0.9012	0.6628	0.3419	0.7654	0.6315
Proposed	0.0227	63.4917	0.9465	0.7429	0.4423	0.7245	0.6752

Table 5: Comparative quantitative evaluation amid the reported methods and proposed RGCNN for T2 Brain MR image with 9% noise variance

Methods	**Parameters**						
	MSE	PSNR	SSIM	UQI	CP	NAE	PSI
FPDE[18]	0.4603	35.6897	0.7394	0.7314	0.4622	0.7236	0.314
NLM [23]	0.5713	37.2431	0.72521	0.7121	0.4523	0.7762	0.4215
WF [21]	0.6213	33.9214	0.7424	0.7245	0.4432	0.7923	0.4682
MCD [16]	0.5413	37.5215	0.81351	0.7931	0.4332	0.5345	0.3213
TV [14]	0.7932	32.1251	0.7215	0.7347	0.4454	0.7632	0.4632
ADMF [20]	0.7927	31.2351	0.7825	0.7281	0.4532	0.7792	0.4627
MCR [22]	0.6942	31.3251	0.7336	0.7267	0.4789	0.7823	0.3829
ADF [15]	0.8231	29.2541	0.8126	0.7512	0.5128	0.7154	0.4820
Gabor [6]	0.1638	61.3452	0.8734	0.9123	0.6347	0.5132	0.5728
Proposed	0.0337	67.8120	0.9439	0.9332	0.6418	0.4923	0.6782

Table 5: Comparative quantitative evaluation amid the reported methods and proposed RGCNN for T2 Brain MR image with 9% noise variance

Methods	**Parameters**						
	MSE	PSNR	SSIM	UQI	CP	NAE	PSI
FPDE[18]	0.6959	38.5121	0.7932	0.5725	0.4721	0.8125	0.4789
NLM [23]	0.6923	38.2925	0.7987	0.5582	0.4697	0.8415	0.5629
WF [21]	0.5939	34.545	0.8051	0.5681	0.4645	0.8523	0.6351
MCD [16]	0.3251	45.6542	0.8123	0.5515	0.5097	0.7799	0.6692
TV [14]	0.3351	44.5191	0.7652	0.5219	0.4698	0.8498	0.7539
ADMF [20]	0.3259	43.8921	0.7753	0.5492	0.5489	0.6125	0.7792
MCR [22]	0.3315	44.6129	0.8949	0.5629	0.5792	0.6561	0.7159
ADF [15]	0.2519	47.9219	0.7859	0.6249	0.5395	0.7921	0.6295
Gabor [6]	0.0692	57.982	0.9124	0.7492	0.7742	0.5925	0.7215
Proposed	0.0551	65.2952	0.9432	0.8991	0.8592	0.5395	0.8954

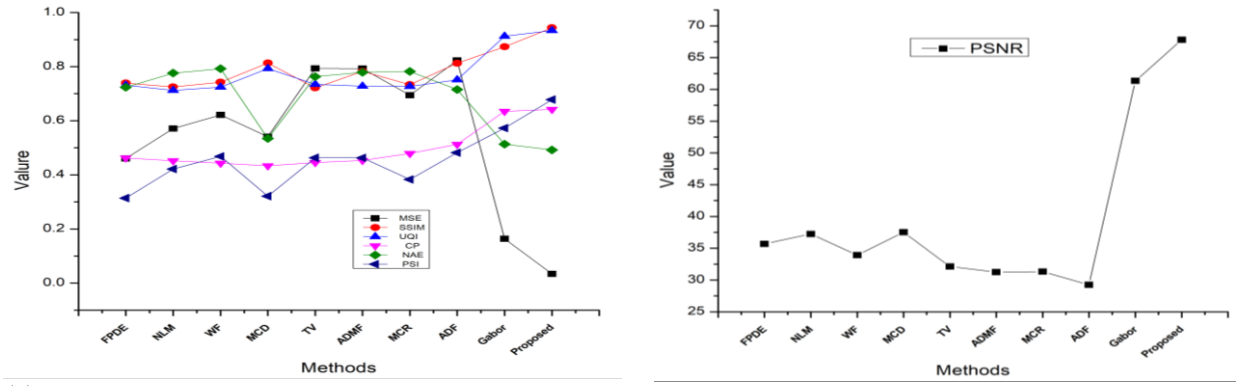

(a) (b)

Figure 10: Line plot comparing the variables in Table 3 with respect to T1 images (a) shows the values MSE, CP, NAE, UQI, SSIM and PSI respectively; (b) illustrates PSNR

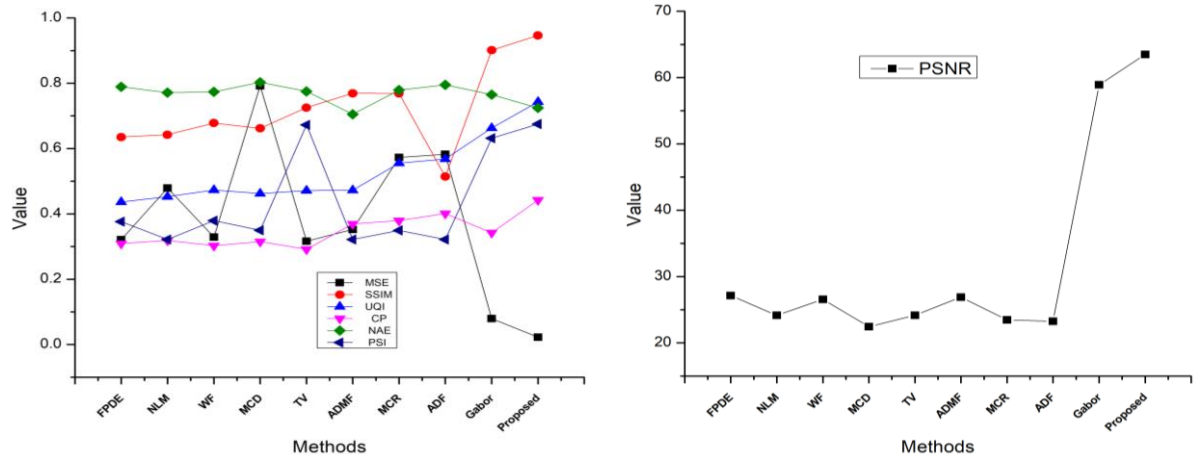

(a) (b)

Figure 11: Line plot comparing the variables in Table 4 with respect to T2 images (a) shows the values MSE, CP, NAE, UQI, SSIM and PSI respectively; (b) illustrates PSNR

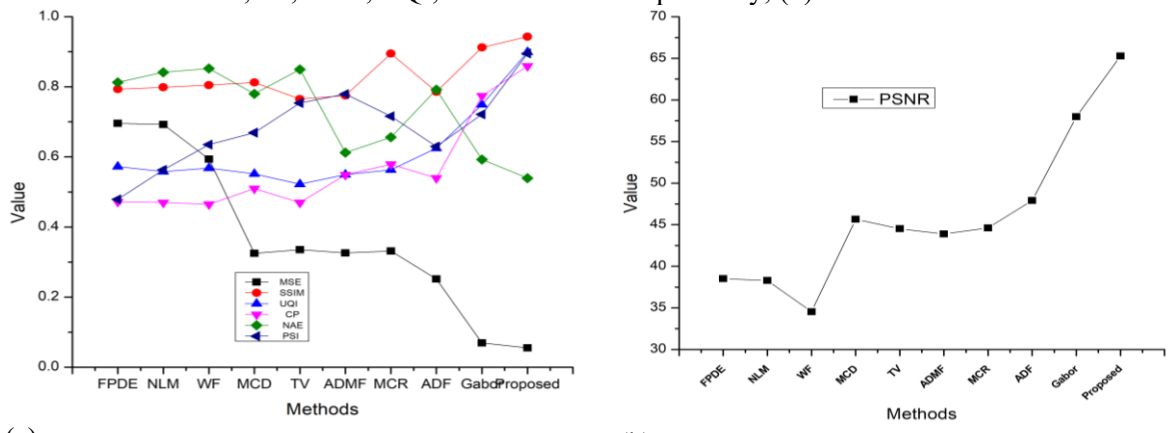

(a) (b)

Figure 12: Line plot comparing the variables in Table 5 with respect to TD images (a) shows the values MSE, CP, NAE, UQI, SSIM and PSI respectively; (b) illustrates PSNR;

6. Conclusion

The primarily objective of the present work was to restore, denoise and enhance the brain MRI images which is usually affected by Rician noise. The objective was accomplished with the aid of the proposed Reshaped Gabor Convolutional Neural Network. The RGCNN combines the attributes of conventional neural Network and Gabor filter kernels). The following modification had been implemented in order to the develop the RGCNN. Thus, both the modifications deliver a single framework for restoration, denoising and

enhancement of brain MRI images instead of performing separately.

The performance of the proposed RGCNN was measured on the 9% noise variance of T1, T2 and PD brain image respectively. The dataset was collected from the Brain web MRI database. The performance was demonstrated in terms of qualitative as well as quantitative study. The qualitative study was used to exemplify the improvement in image quality which was obtained by the proposed RGCNN. Furthermore, the quantitative study was articulated with respect to the metrics of FRAP, HVSAP, and NRAP to measure the efficiency of the proposed RGCNN. The metrics like MSE, PSNR, CP, and NAE were employed as FRAP. UQI and SSIM were utilized as the parameters of HVSAP. The NRAP assessments parameters was cast-off in terms of PSI. Moreover, the performance of the proposed IDAEHBF was also presented in the form of comparative study. The existing methods like FPDE[26], NLM [20], WF [17], MCD [27], TV [12], ADMF [15], MCR [18], ADF [13] and Gabor [6] were used for the comparative study. Based on both qualitative and quantitative studies, it has been found that the suggested RGCNN is the best way to restore, denoise, and improve MRI images with Rician noise while keeping their edges and boundaries. The RGCNN results can be used to find the area of interest for image segmentation as well as to improve the accuracy of the feature extraction and classification processes.

References

1. C. R. Madan, "Advances in studying brain morphology: The benefits of open-access data," *Front. Hum. Neurosci.*, vol. 11, p. 405, 2017.
2. A. Griffa, P. S. Baumann, J.-P. Thiran, and P. Hagmann, "Structural connectomics in brain diseases," *Neuroimage*, vol. 80, pp. 515–526, 2013.
3. J. C. Richardson, R. W. Bowtell, K. Mäder, and C. D. Melia, "Pharmaceutical applications of magnetic resonance imaging (MRI)," *Adv. Drug Deliv. Rev.*, vol. 57, no. 8, pp. 1191–1209, 2005.
4. H. M. Golshan and R. P. R. Hasanzadeh, "A modified Rician LMMSE estimator for the restoration of magnitude MR images," *Optik (Stuttg).*, vol. 124, no. 16, pp. 2387–2392, 2013, doi: 10.1016/j.ijleo.2012.07.001.
5. Z.-P. Liang and P. C. Lauterbur, *Principles of magnetic resonance imaging*. SPIE Optical Engineering Press Bellingham, 2000.
6. V. Kumar and S. Srivastava, "Performance analysis of reshaped Gabor filter for removing the Rician distributed noise in brain MR images," *Proc. Inst. Mech. Eng. Part H J. Eng. Med.*, vol. 236, no. 8, pp. 1216–1231, 2022.
7. R. B. Yadav, S. Srivastava, and R. Srivastava, "An efficient PDE-Based nonlinear filter adapted to Rician noise for restoration and enhancement of magnetic resonance images," in *2016 1st India International Conference on Information Processing (IICIP)*, 2016, pp. 1–5.
8. S. Luan, C. Chen, B. Zhang, J. Han, and J. Liu, "Gabor convolutional networks," *IEEE Trans. Image Process.*, vol. 27, no. 9, pp. 4357–4366, 2018.
9. R. Srivastava, J. R. P. Gupta, H. Parthasarthy, and S. Srivastava, "PDE based unsharp masking, crispening and high boost filtering of digital images," *Commun. Comput. Inf. Sci.*, vol. 40, pp. 8–13, 2009, doi: 10.1007/978-3-642-03547-0_2.
10. P. Coupé, J. V. Manjón, E. Gedamu, D. Arnold, M. Robles, and D. L. Collins, "Robust Rician noise estimation for MR images," *Med. Image Anal.*, vol. 14, no. 4, pp. 483–493, 2010, doi: 10.1016/j.media.2010.03.001.
11. J. Lu, J. Tian, L. Shen, Q. Jiang, X. Zeng, and Y. Zou, "Rician Noise Removal via a Learned Dictionary," *Math. Probl. Eng.*, vol. 2019, 2019, doi: 10.1155/2019/8535206.
12. B. Zhang, X. Wang, Y. Li, and Z. Zhu, "A new difference of anisotropic and isotropic total variation regularization method for image restoration," *Math. Biosci. Eng.*, vol. 20, no. 8, pp. 14777–14792, 2023.
13. R. R. Kumar, A. Kumar, and S. Srivastava, "Anisotropic Diffusion Based Unsharp Masking and Crispening for Denoising and Enhancement of MRI Images," *2020 Int. Conf. Emerg. Front. Electr. Electron. Technol. ICEFEET 2020*, pp. 0–5, 2020, doi: 10.1109/ICEFEET49149.2020.9186966.
14. R. Srivastava, S. Srivastava, and R. B. Yadav, "Identification and removal of different categories of noises from magnetic resonance image using hybrid partial differential equation-based filter," *Int. J. Digit. Signals Smart Syst.*, vol. 1, no. 2, p. 87, 2017, doi: 10.1504/ijdsss.2017.10008982.
15. M. Redhya and K. S. Kumar, "Refining PD classification through ensemble bionic machine learning architecture with adaptive threshold based image denoising," *Biomed. Signal Process. Control*, vol. 85, p. 104870, 2023.
16. D. Lee, C.-S. Yun, S.-H. Kang, M. Park, and Y. Lee, "Performance evaluation of 3D median modified Wiener filter in brain T1-weighted

magnetic resonance imaging," *Nucl. Instruments Methods Phys. Res. Sect. A Accel. Spectrometers, Detect. Assoc. Equip.*, vol. 1047, p. 167779, 2023.

17. K. Singh and R. Kumar, "BRAIN MRI IMAGE DENOISING USING FILTERING APPROACHES".
18. K. Ali, A. N. Qureshi, M. S. Bhatti, A. Sohail, M. Hijji, and A. Saeed, "De-Noising Brain MRI Images by Mixing Concatenation and Residual Learning (MCR).," *Comput. Syst. Sci. Eng.*, vol. 45, no. 2, 2023.
19. A. Kumar and S. Srivastava, "Restoration and enhancement of breast ultrasound images using extended complex diffusion based unsharp masking," *Proc. Inst. Mech. Eng. Part H J. Eng. Med.*, vol. 236, no. 1, pp. 12–29, 2022.
20. P. Thakur, N. Syamala, Y. Karuna, and S. Saritha, "Performance Analysis of IIC techniques for Brain MR-images," in *2023 10th International Conference on Signal Processing and Integrated Networks (SPIN)*, 2023, pp. 351–357.
21. S. Kollem, K. R. Reddy, and D. S. Rao, "A novel diffusivity function-based image denoising for MRI medical images," *Multimed. Tools Appl.*, pp. 1–33, 2023.
22. P.-H. Dinh, "A novel approach based on marine predators algorithm for medical image enhancement," *Sens. Imaging*, vol. 24, no. 1, p. 6, 2023.
23. C. A. Cocosco, "Brainweb: Online interface to a 3D MRI simulated brain database.," *(No Title)*, 1997.
24. A. Kumar and S. Srivastava, "Restoration and enhancement of breast ultrasound images using extended complex diffusion based unsharp masking," *Proc. Inst. Mech. Eng. Part H J. Eng. Med.*, p. 09544119211039317, 2021.
25. A. Kumar, P. Kumar, and S. Srivastava, "A skewness reformed complex diffusion based unsharp masking for the restoration and enhancement of Poisson noise corrupted mammograms," *Biomed. Signal Process. Control*, vol. 73, no. August 2021, p. 103421, 2022, doi: 10.1016/j.bspc.2021.103421.
26. R. B. Yadav, S. Srivastava, and R. Srivastava, "An efficient PDE-Based nonlinear filter adapted to Rician noise for restoration and enhancement of magnetic resonance images," *India Int. Conf. Inf. Process. IICIP 2016 - Proc.*, pp. 0–4, 2017, doi: 10.1109/IICIP.2016.7975339.
27. R. Srivastava, S. Srivastava, and R. B. Yadav, "Modified complex diffusion based nonlinear filter for restoration and enhancement of magnetic resonance images," *Int. J. Biomed. Eng. Technol.*, vol. 23, no. 1, p. 19, 2017, doi: 10.1504/ijbet.2017.10003042.